Prospects of mass measurements for neutral MSSM Higgs bosons in the intense-coupling regime at a linear collider

E. Boos [a,b], V. Bunichev [a], A. Djouadi [c,d], H.J. Schreiber [e]

[a] *Skobeltsyn Institute of Nuclear Physics, MSU, 119992 Moscow, Russia*
[b] *Fermilab, P.O. Box 500, Batavia, IL 60510-0500, USA*
[c] *LPT, Université Paris-Sud & UMR8627-CNRS, Bt. 210, F-91405 Orsay, France*
[d] *LPMT, Université de Montpellier II, F-34095 Montpellier cedex 5, France*
[e] *DESY, Deutsches Elektronen-Synchrotron, D-15738 Zeuthen, Germany*

Abstract

We analyze the prospects for detecting the three neutral Higgs bosons of the Minimal Supersymmetric extension of the Standard Model in the intense-coupling regime at e^+e^- colliders. Due to the small mass differences between the Higgs states in this regime and their relative large total decay widths, the discrimination between the particles is challenging at the LHC and in some cases even impossible. We propose to use the missing mass technique in the Higgs-strahlung process in e^+e^- collisions to distinguish between the two CP-even Higgs eigenstates h and H, relying on their $b\bar{b}$ decay in the $b\bar{b}\ell^+\ell^-$ event sample. Ah and AH associated production is then studied in the 4b-jet event sample to probe the CP-odd A boson. At collider energies $\sqrt{s} \simeq 300$ GeV and an integrated luminosity of 500 fb^{-1}, accuracies in the mass measurement of the CP-even Higgs bosons are expected to range from 100 to 300 MeV, while for the CP-odd A boson, accuracies of less than 500 MeV can be obtained.

In the Minimal Supersymmetric Standard Model (MSSM), two Higgs doublets are needed to break the electroweak symmetry and therefore, there are five physical Higgs states: two CP-even Higgs particles h and H, a CP-odd or pseudoscalar Higgs boson A,

and two charged Higgs particles $H^\pm$ [1]. The intense-coupling regime [2,3] is characterized by a rather large value of the ratio of the vacuum expectation values of the two doublet fields, $\tan\beta = v_2/v_1 \gtrsim 10$, and a mass for the pseudoscalar A boson that is close to the maximal (minimal) value of the CP-even h (H) boson mass. In such a scenario, an almost mass degeneracy of the neutral Higgs particles occurs, $M_h \sim M_A \sim$

E-mail address: djouadi@mail.cern.ch (A. Djouadi).

$M_H \sim 100$–140 GeV. The couplings of both the CP-even h and H particles to gauge bosons and isospin up-type fermions are suppressed, and their couplings to down-type fermions, in particular, to b-quarks and τ leptons, are strongly enhanced. The interactions of both Higgs particles with fermions therefore approach those of the pseudoscalar Higgs boson for which the couplings to isospin $-\frac{1}{2}$ $(+\frac{1}{2})$ fermions are (inversely) proportional to $\tan\beta$ [and which does not couple to massive gauge bosons as a result of CP invariance]. Because of this enhancement, the branching ratios of the h and H bosons into $b\bar{b}$ and $\tau^{+}\tau^{-}$ final states are by far dominant, with values of $\sim 90\%$ and $\sim 10\%$, respectively, similarly to the pseudoscalar Higgs case. A corollary of this feature is that the total decay widths of the three neutral Higgs particles are rather large, being of the same order as the mass differences.

As discussed in Ref. [3], this leads to a rather difficult situation for the detection of these particles at the LHC. The branching ratios of the interesting decays which allow the detection of the CP-even Higgs bosons, namely $\gamma\gamma$, $WW^{*} \to \ell\ell\nu\nu$ and $ZZ^{*} \to 4\ell$, are too small and prevent serious analyses. The $b\bar{b}$ decay mode has a too large QCD background to be useful. For $\tau^{+}\tau^{-}$ decays, the expected experimental resolution on the invariant mass of the tau system is about 10–20 GeV and thus clearly too large for distinct Higgs particle observation; rather, one would simply observe a relatively broad excess over the background, corresponding to A and h and/or H production. A way out, as suggested in Ref. [3], is to rely on the decays into muon pairs with the Higgs bosons produced in association with $b\bar{b}$ pairs, $gg/q\bar{q} \to b\bar{b} + \Phi$ with $\Phi = h, H$ and A; see also Ref. [4]. Although the decay is rare, BR$(\Phi \to \mu^{+}\mu^{-}) \sim 3.3 \times 10^{-4}$, the dimuon mass resolution is expected to be as good as 1 GeV, i.e., comparable to the Higgs total widths for $M_{\Phi} \sim 130$ GeV.[1] However, even in this case, it is

possible to resolve only two Higgs peaks in favorable situations. In general, the detection of the three individual Higgs bosons is very challenging, and in some cases even impossible at the LHC.[2]

In $e^{+}e^{-}$ collisions [6], the CP-even Higgs bosons can be produced in the Higgs-strahlung, $e^{+}e^{-} \to Z + h/H$, and in the vector-boson fusion, $e^{+}e^{-} \to \nu\bar{\nu} + h/H$, processes. The CP-odd particle cannot be probed in these channels due to its zero-couplings to gauge bosons at tree level, but it can be produced in association with the h or H bosons in the reactions $e^{+}e^{-} \to A + h/H$. Earlier studies [7] indicated that the vector boson fusion processes are difficult to use in this context, as the full final state cannot be reconstructed. In turn, the Higgs-strahlung and the Higgs pair production processes, as will be demonstrated in this Letter, have a great potential to explore the individual h, H and A states in the intense-coupling regime and to allow the measurement of their masses.

The cross sections for the Higgs-strahlung and pair production processes are mutually complementary coming either with a coefficient $\sin^{2}(\beta - \alpha)$ or $\cos^{2}(\beta - \alpha)$, with α being the mixing angle in the CP-even Higgs sector:

$$\sigma\left(e^{+}e^{-} \to Z + h/H\right) = \sin^{2}/\cos^{2}(\beta - \alpha)\sigma_{\mathrm{SM}},$$
$$\sigma\left(e^{+}e^{-} \to A + h/H\right) = \cos^{2}/\sin^{2}(\beta - \alpha)\bar{\lambda}\sigma_{\mathrm{SM}},$$

where σ_{SM} is the SM Higgs cross section in the strahlung process and $\bar{\lambda} \sim 1$ for $\sqrt{s} \gg M_{A}$ accounts for P-wave suppression near the kinematical threshold for the production of two spin-zero particles. Since σ_{SM} is rather large, being of the order of 50–100 fb for a Higgs boson with a mass ~ 130 GeV at a c.m. energy $\sqrt{s} \sim 300$–500 GeV, the production and the detection of the three neutral Higgs bosons should be straightforward for an integrated luminosity of $\int \mathcal{L} \sim 0.5$–1 ab^{-1}, as expected at future linear $e^{+}e^{-}$ colliders such as TESLA [7].

In Fig. 1, the production cross sections for the Higgs-strahlung and Higgs pair production of the neutral Higgs particles are shown as a function of the

---

[1] The Higgs-strahlung and vector-boson fusion processes for the production of the h and H bosons, as well as associated production of the three neutral Higgs particles with top quarks, will have smaller cross sections than in the SM due to the suppressed couplings of the particles involved. The production of the three Higgs particles in the gluon–gluon process, $gg \to \Phi \to \mu^{+}\mu^{-}$, although bearing large rates will suffer from the huge Drell–Yan $pp \to \gamma^{*}, Z^{*} \to \mu^{+}\mu^{-}$ background process [3].

[2] An alternative possibility at the LHC is diffractive Higgs production [5] where, based on the recoil mass technique, very good proton beam energy resolution and precise luminosity measurements are crucial to resolve the Higgs signals and perform accurate mass determinations.
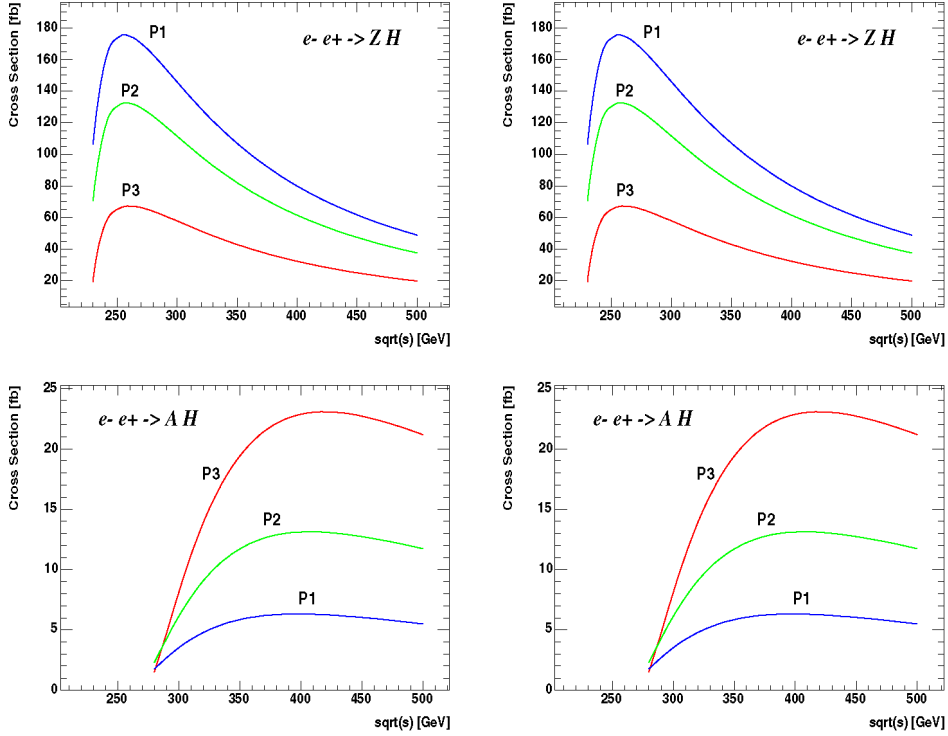
Fig. 1. The production cross sections for the Higgs-strahlung (upper plots) and Higgs pair processes (lower plots) for the MSSM parameter points P1, P2, and P3 with $M_A = 125, 130, 135$ GeV and $\tan\beta = 30$ in the maximal mixing scenario.

c.m. energy. We have chosen the same three representative scenarios P1, P2 and P3 discussed in Ref. [3]: $\tan\beta = 30$ and $M_A = 125, 130$ and 135 GeV. The maximal mixing scenario where the trilinear Higgs-stop coupling is given by $A_t \simeq \sqrt{6}M_S$ with the common stop masses fixed to $M_S = 1$ TeV has been adopted; the other SUSY parameter will play only a minor role and have been set to 1 TeV, while the top quark mass is fixed[3] to $m_t = 175$ GeV. The resulting Higgs masses, couplings and branching ratios shown in Table 1 have been obtained using the program HDECAY [8] in which the routine FeynHiggsFast [9] is used for the implementation of the radiative corrections. As apparent from Fig. 1, values of $\sqrt{s}$ not too far above the kinematical thresholds of these reactions are favored within our scenarios with $M_\Phi \sim 130$ GeV, since the cross sections scale like $1/s$

Table 1

Masses, total decay widths (in GeV) and some decay branching ratios of the MSSM neutral Higgs bosons for the points P1, P2 and P3 with $\tan\beta = 30$

Point	Φ	M_Φ	Γ_Φ	BR($b\bar{b}$)	BR($\tau^+\tau^-$)
P1	h	123.3	2.14	0.905	0.093
	A	125.0	2.51	0.905	0.093
	H	134.3	0.36	0.900	0.094
P2	h	127.2	1.73	0.904	0.093
	A	130.0	2.59	0.904	0.094
	H	135.5	0.85	0.900	0.094
P3	h	129.8	0.97	0.903	0.094
	A	135.0	2.67	0.904	0.094
	H	137.9	1.69	0.902	0.095

as the processes are mediated by s-channel gauge boson exchange. We will thus choose to operate the e^+e^- collider at $\sqrt{s} = 300$ GeV in the present analysis, as the production cross sections are large enough for all cases considered.

The Higgs-strahlung processes offers the most promising way to discriminate between the two CP-
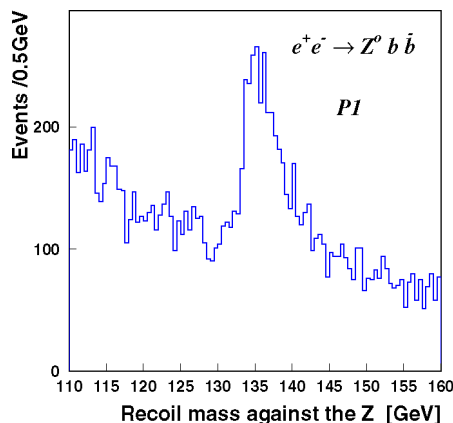
Fig. 2. The recoil mass distribution for signal and background including ISR, beamstrahlung and detector smearing for the parameter point P1 before cuts and b-tagging.

even Higgs particles, since the pseudoscalar boson A is not involved. For the SM Higgs boson, as was widely demonstrated, the recoil mass technique in both leptonic and hadronic Z decays allow very precise determination of its mass; for instance, an accuracy of ~ 40 MeV for a mass of ~ 120 GeV can be achieved [7]. In the intense-coupling scenario, where the two scalar h and H bosons are close in mass and are often produced with different rates, some of them being small, the impact of initial state radiation (ISR) and beamstrahlung is important and should be carefully taken into account. We have performed a detailed simulation, including the signal and all the main background reactions using the program package CompHEP [10] interfaced [11] with PYTHIA [12], as well as a simulation of the detector response with the code SIMDET [13]. The analysis reveals that the most promising way for measuring the h and H boson masses is to select first the $\ell^+\ell^- b\bar{b}$ event sample $(\ell = e/\mu)$, followed by the recoil Z mass technique. However, without cuts and b-quark tagging, the signals from the h and H bosons cannot be resolved, as illustrated in Fig. 2 in the case of the parameter point P1.

If some realistic b-tagging is applied and the surviving $b\bar{b}\ell^+\ell^-$ events are required to pass the following cuts: (i) the dilepton invariant mass is within $M_{\ell^+\ell^-} = 90 \pm 6$ GeV, i.e., compatible with the Z boson, (ii) each jet energy has $E_j \geqslant 12$ GeV, (iii) the angle between two jets is $\angle(j_1, j_2) \geqslant 95$ degrees,

the separation of the two Higgs signal peaks is possible and the masses are accessible. Simulation results for the case of TESLA, as an example, and for the MSSM parameter points P1, P2 and P3 are shown in Fig. 3. The selection efficiencies are found to be 68% for the signal reaction, while they are at the level of 22% for the $\ell^+\ell^- b\bar{b}$, 6.4% for the $\ell^+\ell^- c\bar{c}$ and 0.1% for the $\ell^+\ell^- q\bar{q}$ $(q = u, d, s)$ background processes.

As evident from Fig. 3, the masses of the h and H particles can be determined with accuracies of the order of 100–300 MeV at a 300 GeV collider energy and with 500 fb^{-1} accumulated luminosity. Such uncertainties in the mass measurements are significantly smaller than the typical mass differences between the two Higgs states. They are however larger than the corresponding accuracy for the SM Higgs boson. At higher c.m. energies, the mass determination will be significantly worse as a consequence of the smaller production cross sections, degraded energy resolution of the more energetic leptons and the stronger impact of ISR and beamstrahlung. It would become very difficult to resolve the h and H signals as is demonstrated in Fig. 4 for $\sqrt{s} = 500$ GeV and two times larger integrated luminosity of $\int \mathcal{L} = 1$ ab^{-1}. Here, only the Higgs signal events are shown.

Once the h and H boson masses are known from the recoil mass technique, attention should be directed to the mass determination of the A particle which can be probed in the complementary pair production channels $e^+e^- \rightarrow A + h/H$. This can be achieved either via the reconstruction of the $b\bar{b}$ and/or $\tau^+\tau^-$ invariant masses or through a threshold scan. The first method has been discussed in Ref. [14] for the production of heavier Higgs bosons in the decoupling limit $M_A \sim M_H \gg M_Z$, in the reaction $e^+e^- \rightarrow HA \rightarrow 4b$ at $\sqrt{s} = 800$ GeV. Accuracies of about 100 MeV for the H/A masses were obtained sufficiently above the reaction thresholds using the dominant $b\bar{b}b\bar{b}$ and $b\bar{b}\tau^+\tau^-$ final states [15].

In the intense-coupling regime, the three neutral Higgs bosons contribute to the $b\bar{b}b\bar{b}$ and $b\bar{b}\tau^+\tau^-$ final state signals. Since typical b-jet energy resolutions are close to or somewhat larger than the Higgs mass differences, it is challenging to discriminate between the $A \rightarrow b\bar{b}$ and the $h/H \rightarrow b\bar{b}$ decays, as illustrated in Fig. 5 where all possible $b\bar{b}$ mass combinations for
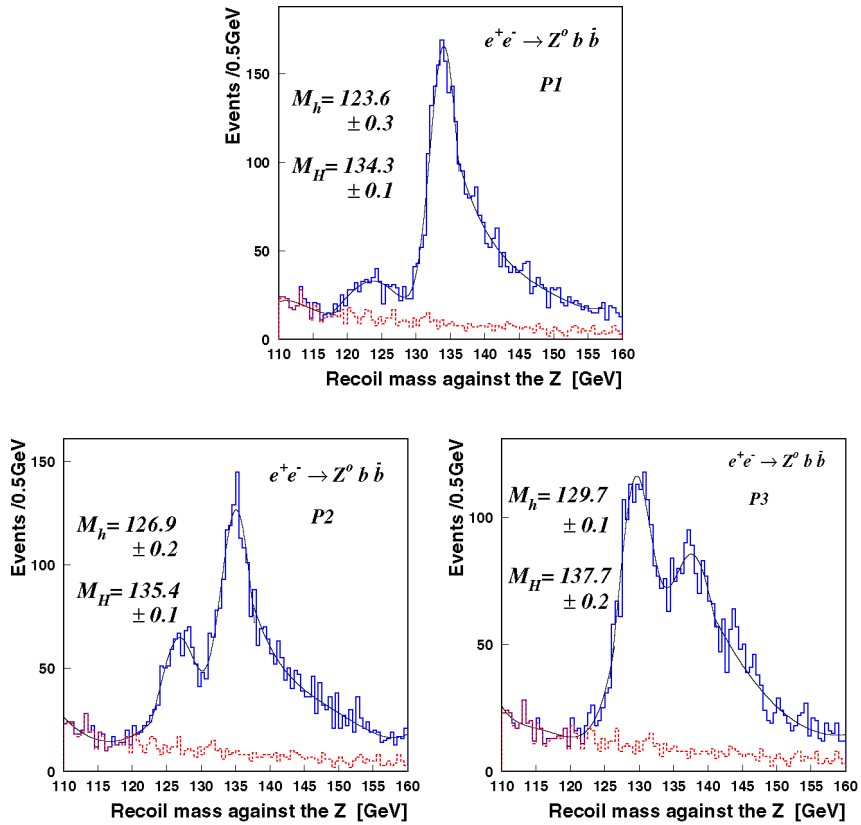
Fig. 3. The recoil mass distributions for the sum of signal and background including ISR, beamstrahlung and detector smearing for the parameter points P1, P2, P3 after cuts and b-tagging. The background is separately shown as dashed histogram. The solid line is the result of a fit, with values for M_h and M_H as indicated.
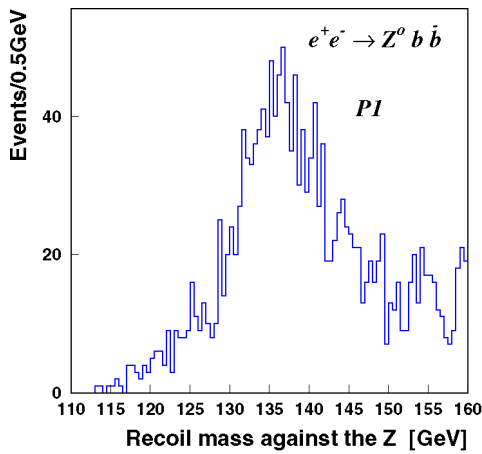

Fig. 4. The recoil mass distribution for signal events in $e^+e^- \rightarrow Zb\bar{b}$ at $\sqrt{s} = 500$ GeV and $\int \mathcal{L} = 1$ ab^{-1} for the parameter point P1.
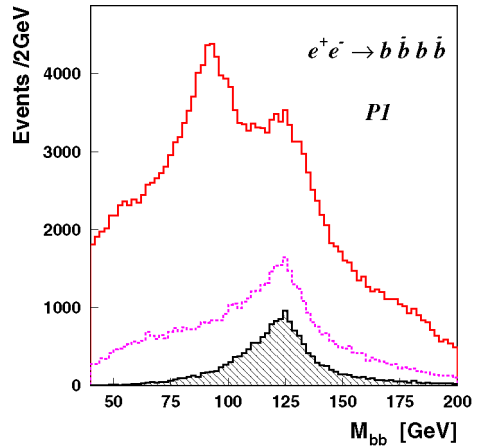

Fig. 5. $b\bar{b}$ invariant mass distributions for the combined signal and total background (top), for the sum of signal and combinatorial background (dashed) and only the signal (shaded histogram) for the parameter point P1.

the signal and the sum of signal and background events are shown for the parameter point P1 as an illustration.

To associate the correct $b\bar{b}$ mass combination to the A and h/H boson decay into $4b$ final state events, we use the "combinatorial mass difference" method. After selecting $4b$-jet events by means of b-tagging, we consider all three possible combinations of 2 b-jet pairs. Only one of them is the "physical" combination where both b-quarks in each pair correspond to one of the decaying Higgs particles, while the other two combinations are combinatorial background.

Because of the well defined kinematics in the process $e^+e^- \to A + h/H \to b\bar{b}b\bar{b}$, the angle between two b-jets in the Higgs decay

$$\angle(b\bar{b}) \simeq 2 \times \arctan\left(2 \times \sqrt{\frac{M_\Phi^2 - 4m_b^2}{s - 4M_\Phi^2}}\right)$$
$$(\Phi = A, h, H), \tag{1}$$

is about $115°$ for our parameter set and independent of the Higgs particles since their masses are almost degenerate. The influence of ISR and beamstrahlung leads to some smearing of the corresponding angular distribution as shown in the left-hand side of Fig. 6. A sharp distribution is evident for the "correct" or signal b-jet pair, while the combinatorial b-jet background pairing leads to a flat distribution.

In addition, b-jet pairs originating from Higgs decays are more centrally produced than the combinatorial background, as evident from the right-hand side of Fig. 6. Thus, the separation of the "physical" combinations from the combinatorial background might be achieved by means of the following cuts: (i) $-0.95 < \cos\theta_{b_1b_2} < -0.3$ and (ii) $|\cos\theta_{bb\text{-pair}}| < 0.7$, where $\theta_{b_1b_2}$ is the angle between two b-jets and $\theta_{bb\text{-pair}}$ the polar angle of the $b\bar{b}$ system. The "physical pairs" are selected with an efficiency of about 85%, whereas the background combinations are selected with an efficiency of about 20%.

In the discrimination between Ah and AH production, we use the average mass, $\bar{M} = \frac{1}{2}(M_1 + M_2)$, where M_1 and M_2 are randomly chosen among two invariant masses of 2 b-jets in the event sample after cuts. If $\bar{M}$ is closer to the known mass of the h boson measured by the recoil mass technique, we associate the $4b$-jet final state to $e^+e^- \to Ah$ production, otherwise it is associated to $e^+e^- \to AH$.

Finally, the selection of the pseudoscalar boson A from the Ah and AH pairing relies on some probability estimation based on the function

$$\mathcal{P} = \frac{1}{2} + \frac{1}{2} \times \frac{M_2 - M_1}{M_2 + M_1}. \tag{2}$$

If, for instance, the former step favors Ah production for a particular $4b$-jet event, the function $\mathcal{P}$ gives the probability that the first chosen invariant mass M_1 is the mass of the h boson. This probability value is compared with a uniformly distributed random number r in the range $[0, 1]$. If $\mathcal{P} > r$, the association $M_h = M_1$ and $M_A = M_2$ is performed, whereas for the opposite case $\mathcal{P} < r$, we assign $M_h = M_2$ and $M_A = M_1$. The same procedure is applied if AH pair production has been favored in the first step. Resulting $b\bar{b}$ mass spectra for the MSSM parameter points P1, P2 and P3 are shown in Fig. 7. Only the $2b$-jet masses which have been assigned to the pseudoscalar A boson are displayed, and all $4b$-jet background sources have been taken into account.

As fits to these histograms revealed, the mass of the pseudoscalar Higgs boson A can be measured with an accuracy of 300 to 500 MeV, once the measured masses of the h and H particles with their corresponding errors have been taken into account. Such experimental accuracies, although larger than those for the SM Higgs boson, are smaller than the typical mass differences $M_A - M_h$ or $M_H - M_A$ in the chosen scenarios.

One may expect a more precise determination of the mass values for the A boson by measuring the $e^+e^- \to A + h/H$ production cross sections near the respective kinematical thresholds, where the cross sections rise as $\sigma \sim \beta^3$ with $\beta \sim \sqrt{1 - 4M_A^2/s}$. This is very similar to scalar lepton pair production in e^+e^- collisions, $e^+e^- \to \tilde{\ell}\tilde{\ell}$ in supersymmetric models, which has many common characteristics with the process discussed here. Indeed, it has been shown [16] that slepton masses of the order of 100 GeV can be measured with an accuracy of less than 0.1% in a threshold scan. Whether this holds also true for $e^+e^- \to A + h/H$ production in the intense-coupling regime (the production cross sections are smaller but the final states are cleaner) has to be studied in detail, including ISR and beamstrahlung. This study is however beyond the scope of this Letter.
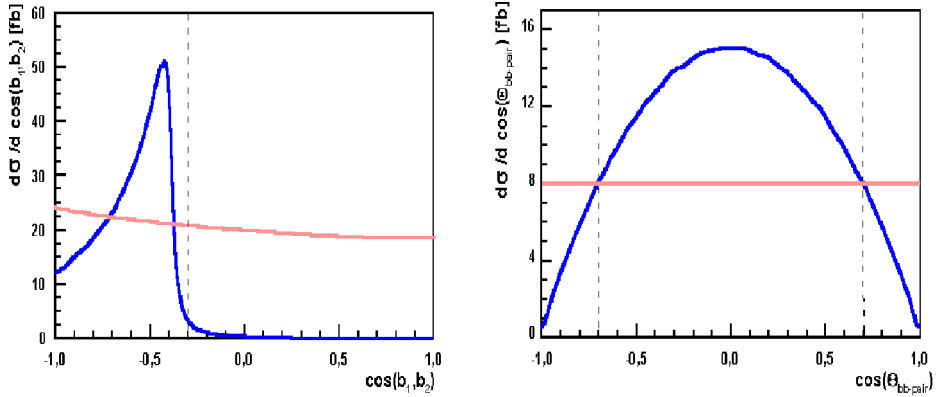
Fig. 6. The differential distributions of the angle between two *b*-jets for the "physical" and combinatorial background combinations (left) and the polar angular distribution for *b*-jet pairs (right). The background concerns the flat distributions in either case.
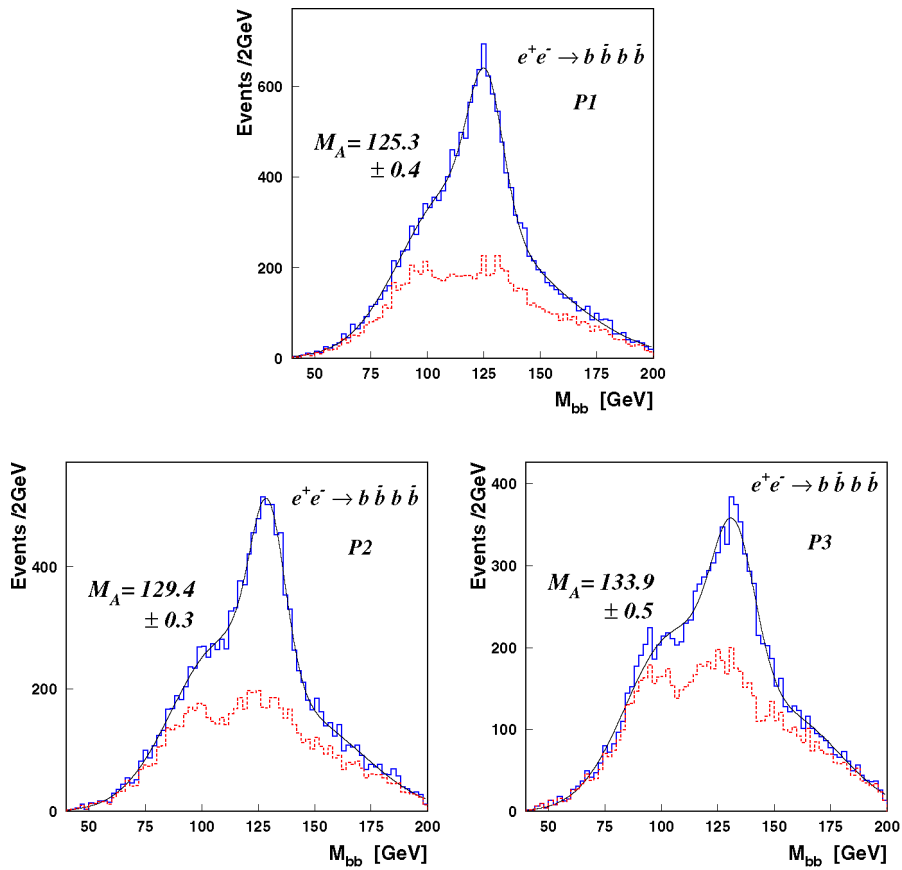

Fig. 7. The two *b*-jet invariant mass associated to the pseudoscalar *A* boson after cuts and the selection procedure for the parameter points P1, P2 and P3. The top histogram represents signal plus background, while the dashed histogram the background only. The solid line is the result of a fit, with values for M_A as indicated.

In conclusion, the intense-coupling regime in the MSSM Higgs sector, in which $\tan\beta$ is rather large and the three neutral h, H and A Higgs particles have comparable masses, is a difficult scenario to be resolved completely at the LHC. In e^+e^- collisions, thanks to the clean environment and to the complementarity of the available production channels, the separation of the three states is possible. The Higgs-strahlung processes allows first to probe the h and H bosons and to measure their masses from the recoiling mass spectrum against the Z boson; the best results are obtained by selecting the $b\bar{b} + \ell^+\ell^-$ event sample and imposing b-jet tagging. Then, associated CP-even and CP-odd Higgs production would allow to probe the pseudoscalar A boson by direct reconstruction of its decay products. At collider energies $\sqrt{s} \simeq 300$ GeV and with integrated luminosities of 500 fb^{-1}, accuracies for the measurement of the masses of the three neutral Higgs particles are expected to range from 100 to 500 MeV, which is smaller than the typical Higgs mass differences in this scheme.

In the study of the intense-coupling regime, the interplay between the LHC and a future linear collider might be very important: on the one hand, any broad peak information observed at the LHC will assist the choice of the appropriate energy at the LC and on the other hand, characteristics of the Higgs states as measured at the linear collider could constrain techniques to access further observables at the LHC such as the gluon–gluon-Higgs couplings and the $\Phi \to \mu^+\mu^-$ branching ratios, as the processes $gg \to \Phi \to \mu^+\mu^-$ might be then possible to detect, a posteriori. Indeed, as shown in Ref. [3], the latter process has a too small signal over background ratio; the precise knowledge of the neutral Higgs boson masses from the ILC would possibly allow to focus on the relevant mass windows to extract the Higgs signal events at the LHC in these channels.

In this Letter, we have concentrated on the MSSM with minimal particle content and in which flavor and CP-symmetry are conserved. As it has been demonstrated, even in this case, a separation of the three close in mass Higgs states is a challenging task. In extensions of this model, the situation might be even more complicated in some regions of the parameter space. For instance, in the MSSM with CP-violating soft SUSY-breaking parameters, the phases of some SUSY parameters will enter the radiative corrections to the Higgs sector and alter the mass and coupling patterns. This could first lead to a closer mass degeneracy of the three neutral Higgs bosons in some cases. In addition, since these particles will have no definite CP quantum numbers, they could all be produced in both the strahlung and pair production processes. Depending on the differences of the masses of the Higgs bosons and on their couplings (in particular those to the Z boson which will control the production cross sections), the detection of the Higgs peaks and the determination of the particle masses might be more challenging than in the MSSM. A detailed analysis, which is beyond the scope of the present Letter, would be required to assess at which extent these measurements can be performed at the LHC and/or at a linear e^+e^- collider.

Acknowledgements

References

[1] For a review on the Higgs sector of the MSSM, see: J.F. Gunion, H.E. Haber, G.L. Kane, S. Dawson, The Higgs Hunter's Guide, Addison–Wesley, Reading, MA, 1990.

[2] E. Boos, A. Djouadi, M. Mühlleitner, A. Vologdin, Phys. Rev. D 66 (2002) 055004.

[3] E. Boos, A. Djouadi, A. Nikitenko, Phys. Lett. B 578 (2004) 384.

[4] V. Barger, C. Kao, Phys. Lett. B 424 (1998) 69;
T. Han, B. McElrath, Phys. Lett. B 528 (2002) 81;
S. Dawson, D. Dicus, C. Kao, Phys. Lett. B 545 (2002) 132.

[5] A. Kaidalov, V. Khoze, A. Martin, M. Ryskin, Eur. Phys. J. C 33 (2004) 261.

[6] J. Ellis, M. Gaillard, D. Nanopoulos, Nucl. Phys. B 106 (1976) 292;
B. Lee, C. Quigg, H. Thacker, Phys. Rev. D 16 (1977) 1519;
J.D. Bjorken, SLAC Rep. 198 (1976);
B. Ioffe, V. Khoze, Sov. J. Part. Nucl. 9 (1978) 50;

J. Ellis, et al., Phys. Rev. D 39 (1989) 844;
A. Djouadi, et al., Z. Phys. C 57 (1993) 569;
A. Djouadi, et al., Z. Phys. C 74 (1997) 93.

[7] TESLA TDR, J.A. Aguilar-Saavedra, et al., hep-ph/0106315.

[8] A. Djouadi, J. Kalinowski, M. Spira, Comput. Phys. Commun. 108 (1998) 56.

[9] S. Heinemeyer, W. Hollik, G. Weiglein, Comput. Phys. Commun. 124 (2000) 76.

[10] A. Pukhov, et al., Report INP-MSU 98-41/542, hep-ph/9908288;
CompHEP Collaboration, E. Boos, et al., hep-ph/0403113.

[11] A.S. Belyaev, et al., hep-ph/0101232;
http://theory.sinp.msu.ru/comphep;
E. Boos, et al., hep-ph/0109068.

[12] T. Sjostrand, L. Lonnblad, S. Mrenna, hep-ph/0108264.

[13] M. Pohl, H.J. Schreiber, hep-ex/0206009.

[14] A. Andreazza, C. Troncon, Report DESY-123-E, p. 417.

[15] K. Desch, T. Klimkovich, T. Kuhl, A. Raspereza, hep-ph/0406229.

[16] G. Blair, H.U. Martyn, Note LC-TH-2000-023, hep-ph/0002290.